Effect of anti-block particles on oxygen transmission rate of SiOx barrier coatings deposited by PECVD on PET films

Pierre Fayet[(a)], Bertrand Jaccoud[(a)], Richard Davis[(b)], Dagmar Klein[(b)]

[(a)]Tetra Pak R&D, Plasma Technology
Tetra Pak (Suisse) SA, CH-1680 Romont, Switzerland
Phone +41 26 651 8619, Fax +41 26 651 8912

[(b)]Mitsubishi Polyester Film GmbH
Rheingaustrasse 190 - 196
65203 Wiesbaden, Germany
Phone +49 611 962 65 23, Fax+49 611 962 92 46

Abstract

The influence of the surface morphology of semi-crystalline poly(ethylene terephthalate) (PET) substrates films on oxygen transmission rate (OTR) and on mechanical properties of ultra thin oxide coatings is analysed, with attention paid to the role surface defects initiated by anti-block particles. Nanometer thick SiOx coatings are deposited by PECVD on three grades of PET films containing pre-determined defect surface densities ranging from 300 to 1800-mm^{-2}. Coating failure is shown to be initiated at defect sites and leads to a decrease of the crack onset strain by a factor of 20% and a lost of barrier by a factor of 3. The failure mechanisms of coatings are determined by means of fragmentation tests and the results are modelled using a constant interfacial strength approach with a Weibull-type probability of fracture.

Introduction

The outstanding mechanical and optical properties give bi-oriented PET (BOPET) films widespread uses in the packaging industry for conditioning numerous varieties of food products. The processability of such films is improved in particular by anti-blocking particles embedded in the polymer melt before film forming stage. These particles induce micron-size protuberances surrounded by a thin polymer skin, forming protrusions of few hundreds of nm height above PET surface. As showed by Sobrinho *et al.*[1] these particles have a negative effect on the barrier properties of thin oxide coatings such as those deposited by plasmas enhanced chemical vapour deposition (PECVD) on PET films[2,3] because they induce sites of barrier defects[1,4] and internal stress of the oxide layer[5,6]. In the early stages of the plasma deposition process molecular radicals, energetic ions and photons interact strongly with the polymer surface, leading to considerable changes of the surface structure, including modifications of the anti-blocking protuberances. As a consequence the overall performances of the oxide-polymer hybrid material are limited. SiOx characteristics such as cohesive strength of the thin oxide layer and its adhesion to the polymer substrate might be strongly modified because these two factors are controlled by the defect structure and internal stress of the oxide and by process induced modifications of the interfacial region and of the polymer substrate[7,8]. It results a lost of barrier against diffusion of oxygen and other gases and aromas.

The aim of this article is to present results on the effects of the anti-blocking particles on oxygen diffusion barrier and on mechanical properties of PECVD SiOx layers in relation with chosen surface density of anti-blocking at the PET film surface. To this end, oxygen transmission rate measurements (OTR) were used to determine oxygen diffusion through SiOx-PET composites and fragmentation tests[9] were applied to measure shifts of the crack onset and changes in adhesion and in cohesion strengths of thin oxide layers.

Experiment

Thin silica coatings (SiOx) were deposited by plasma enhanced chemical vapour deposition from oxygen-diluted hexamethyldisiloxane (HMDSO) vapour on 12-μm BOPET films. Oxide coating thicknesses were determined by XRF centred on the fluorescence signal of silicon atoms (Philips….). For aim of demonstration 9 and 40 nm thick silica coatings were studied. Three types of coextruded, biaxially oriented films, made of polyethylene terephthalate (PET), provided by Mitsubishi Polyester Films, Wiesbaden, were investigated. RNK12 (®Hostaphan RNK, 12-μm), RD12 (®Hostaphan RD, 12-μm) and RDO12 (not commercialised) were chosen because of their different surface topography. While the surface structure of one surface of RD12 and RDO12 were the same as standard RNK12, the functional surface side displayed an extremely regular structure at the polymer surface with very low roughness due to stepped down quantity of anti-blocking particles. The films were characterised by reflection optical microscopy to specify the number density of anti-blocking particles at the polymer surface. Oxygen transmission rates (OTR) were determined by Mocon equipment (Mocon 2/60) for each combination of SiOx coating thickness and PET substrate film.

For determining SiOx cohesive strength and SiOx-PET interfacial shear strength (adhesion strength), *in situ* fragmentation tests were carried out in a Cambridge scanning electron microscope (Stereoscan 240). The samples were mounted in an elongation cell placed in the microscope and were stepwise loaded up to predefined nominal strain levels ε. Coating cracks in SiOx layer initiated when the coating cohesive strength was reached resulting from the transfer of tensile stress of the PET substrate through interfacial shear. The cracks propagate almost instantaneously across the sample width, perpendicular to the tensile direction. At each selected strain, the crack density, defined as the inverse of the average fragment length, was determined by dividing the number of counted cracks on a micrograph by the micrograph length. The result was multiplied by $(1+\varepsilon)$ for taking into account the length opening between fragments.

Results and discussion

Anti-block particles were observed by reflection optical microscopy for taking into account only the particles forming protrusions at the film surface. Fig. 1 shows a 330x490 μm^2 micrograph for each grade of PET films: a) RNK12, b) RD12 and c) RDO12. From these pictures it was obvious that the surface density of particles was a function of the PET film properties and protrusion sizes were distributed over a wide range of diameters. The size distributions are depicted at Fig. 2. On this figure the distributions are shifted up for clarity of plots and the continuous curves are lognormal fits of experimental data. One can see that the particle size was very similar for each type of films with a peak diameter value comprised between 1.0 and 1.5 μm.

Integrating the size distributions provided 1710, 860 and 290 particles per mm^2 for each film quality respectively. These results have to be taken with care because it is known[1] that not all observed protrusions were of nature to generate barrier defects in SiOx coatings.

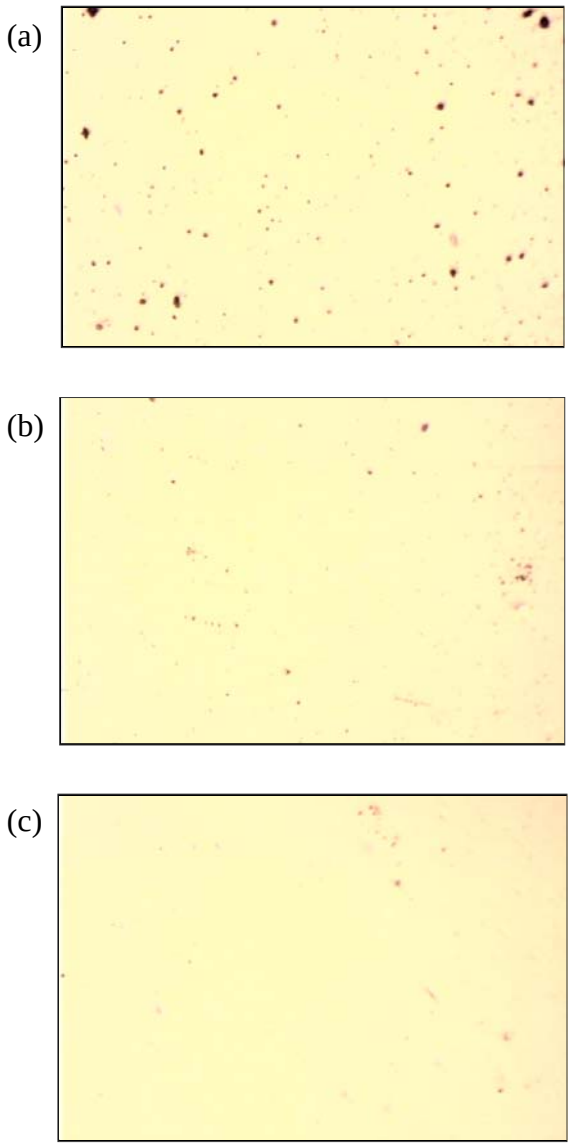

FIG. 1 330x490 μm^2 reflection optical micrographs of RNK12 (a), RD12 (b) and RDO12 (c) BOPET films

The oxygen transmission rates (OTR) were measured for 40-nm thick silica coatings deposited on each of the three types of PET films (Mocon 2/60). The OTRs scaled up following the particles number density at PET surface, given 0.58, 0.39 and 0.21 ± 0.05 (cm^3/m^2/day/atm) for RNK12, RD12 and RDO12 respectively (see Table 1).

The evolution of damage in oxide coatings submitted to uniaxial loading was determined for RNK12 and RDO12. Fig 3(a) compares the crack density as function of nominal strain for the two types of substrates coated with 9-nm thick

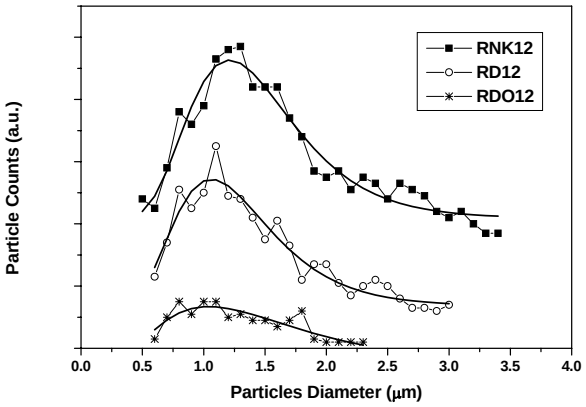

FIG. 2 Size distribution of anti-blocking particles for RNK12, RD12 and RDO12.

SiOx and Fig. 3(b) compares the same for a 40-nm thick SiOx coating. Although the crack density curves of Fig. 3(a) and 3(b) look very similar, the crack onset strain (COS) at the start of the fragmentation process of 9-nm SiOx was found at 3.8% for RNK12 and at 4.8% for RDO12, while the COS for 40-nm SiOx was much lower at 2.3 for RNK12 and 1.9 for RDO12 (see Tables 2 and 3). As already reported[10], SiOx thickness did affect the COS position: thicker coatings fragmented at lower strain than thinner coatings. Hence thick coatings were more fragile than thinner ones. The above data demonstrate that differences in surface density of particles between RNK12 and RDO12 did modify substantially the COS by about 20% for 9-nm SiOx. The other peculiar results were that 1) the crack density at saturation was systematically lower for RDO12 than for RNK12, and 2) the saturation values were dependent on the SiOx thickness, being lower in the case of 40-nm thick SiOx coatings.

Table 1: Particle density and OTR data for a 40-nm SiOx barrier coating deposited by PECVD on PET film substrates.

Film	Particles per mm^{-2}	OTR* (cm^3/m^2/day/atm)
RNK12	1710	0.58 ± 0.1
RD12	860	0.39 ± 0.1
RDO12	290	0.21 ± 0.1

* at 23 °C and 50% R.H.

The interfacial shear strength (IFSS), characterising the oxide-substrate adhesion force, was modelled by stress transfer analysis of the interface. In the case of perfectly plastic interface, the IFSS was found to be proportional to the tensile strength of the oxide coating[9]

$$\tau = \frac{2h_c}{l_c}\sigma_{\max}(l_c)$$

where the critical stress transfer length is defined by $l_c = 0.67 \cdot \bar{l}_{sat}$ for which $\bar{l}_{sat}$ is the average fragmentation length at saturation. The strength $\sigma_{\max}(l_c)$ was modelled using the classical Weibull distribution

$$\sigma_{\max}(l) = \beta\left(\frac{l}{l_0}\right)^{-1/\alpha}\Gamma\left(1+\frac{1}{\alpha}\right)$$

where α is a shape parameter or Weibull modulus, β is a scale parameter, l_0 is a normalising factor taken to be equal to 1 μm and Γ is the gamma function.

The modelled mechanical data for the RNK12 and RDO12 are summarised at Table 2 for 9-nm thick silica coating and at Table 3 for 40-nm thick silica coating.

Table 2: Mechanical properties of 9-nm thick SiOx coating on RNK12 and RDO12.

Film	COS (%)	σ_{max} (GPa)	τ (MPa)
RNK12	3.8 ± 0.05	9.5	137
RDO12	4.8 ± 0.05	7.4	128

Table 3: Mechanical properties of 40-nm thick SiOx coating on RNK12 and RDO12.

Film	COS (%)	σ_{max} (GPa)	τ (MPa)
RNK12	2.3 ± 0.05	2.8	94
RDO12	1.9 ± 0.05	4.7	196

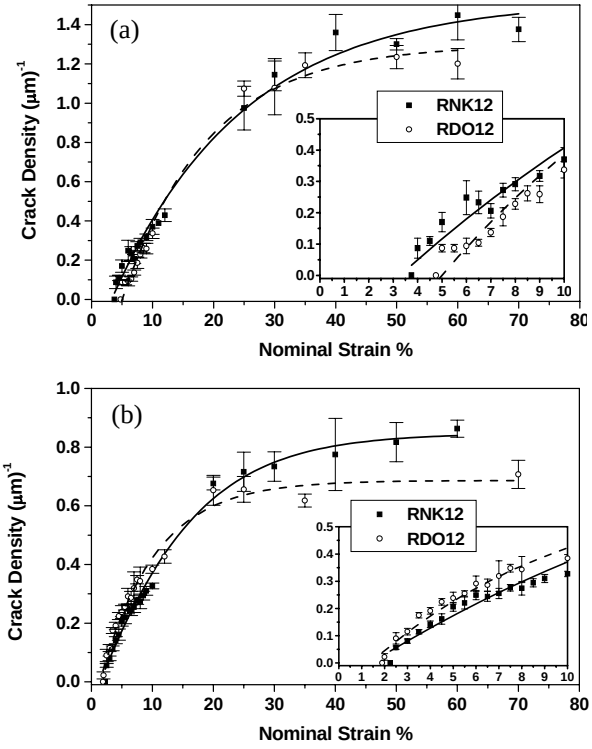

FIG. 3 Crack density vs nominal strain for SiOx coatings of 9-nm thick (a) and 40-nm thick (b) deposited by PECVD on RNK12 and RDO12 bi-

Although tabulated cohesion and adhesion data have to be taken with care due to large error of the about 50%, the IFSS values close to 100 MPa reflected the behaviour of the interfacial region where silica-polymer adhesion results from high density of covalent interactions between the polymer and SiOx formed during plasma deposition process. These interactions involve C-Si and C-O-Si chemical bonds [11,12] and interactions such as hydrogen bonds between silanol groups of the oxide and carboxylic functions of the polymer[13].

Coating cohesion forces in the order of several GPa were function of oxide thickness. This characteristic of thin coatings was already reported for evaporated oxides[14], where the high strength of thin coatings was related to the fact that only volume defects contribute to the strength variation as function of coating thickness.

Conclusion

The oxygen transmission rate (OTR) and the crack onset strain (COS) of plasma enhanced chemical vapour deposited SiOx coatings on bi-oriented PET films were found to be dependent on the presence of anti-blocking particles forming protrusions at the film surface. OTR values were directly proportional to the surface density of anti-blocks while the COS increased up by 20% for substrate with the lower anti-block density. These data are very useful for further converting of the PET/SiOx material in packaging structures since higher barrier means longer shelf life and higher COS allows higher processability of SiOx layer.

The cohesive and adhesive strength were derivate from micro-mechanical modelling of the fragmentation behaviour of PECVD SiOx coatings submitted to uniaxial straining of the coated polymer substrates. The tensile strength of the 9-nm thick SiOx was found to be about twice higher than the 40-nm thick SiOx layer, in agreement with control of fragmentation by volume defects in SiOx.

The interface shear strength, related to adhesion of SiOx on PET, is as high as the bulk shear stress of the polymer, reflecting the presence of covalent bonds at the interface between SiOx layer and PET substrate.

Acknowledgments

The authors wish to thanks Dr. Gil Rochat for valuable discussions.

References

1. A. S. D. S. Sobrinho, G. Czeremuszkin, M. Latreche and M. Wertheimer, Appl. Phys. A: Mater. Sci. Process. **68**, 103 (1999).
2. P. Fayet, C. Holland, B. Jaccoud and A. Roulin, *Proc. 38th SVC Annual Conference* (Society of Vacuum Coater, 1995) pp. 15-16.
3. H. Chatam, Surf. Coat. Technol. **78**, 1 (1996).
4. A. P. Roberts, B. M. Henri, A. P. Sutton, C. R. M. Grovenor, G. A. D. Briggs, T. Miyamoto, M. Kano, Y. Tsukahara and M. Yanaka, J. Membr. Sci. **208**, 75 (2002).
5. Y. Leterrier, Y. Wyser and J.-A. E. Manson, J. Adhes. Sci. and Technol. **15**, 841 (2001).
6. M. Benabdi and A. A. Roche, J. Adhes. Technol. **11**, 281 (1997).
7. G. Rochat, Y. Leterrier, L. Garamszegi, J.-A. E. Manson and P. Fayet, Surf. Coat. Technol. **174-175**, 1029 (2003).
8. G. Rochat, A. Delachaux, Y. Leterrier, J.-A. E. Manson and P. Fayet, Surf. Interf. Anal. **35**,948 (2003).
9. Y. Leterrier, L. Boogh, J. Andersons and J.-A. E. Manson, J. Polym. Sci., part B: Polym. Phys. **35**, 1449 (1997).
10. Y. Leterrier, G. Rochat, P. Fayet and J.-A. E. Manson, *Proc. 41th SVC Annual Conference* (Society of Vacuum Coater, 1998) pp. 429-433.
11. M. Benmalek and H. M. Dunlop, Surf. Coatngs Technol., **76-77**, 821 (1995).
12. J. C. Rotger, J. J. Pireaux, R. Caudano, N. A. Thorne, H. M. Dunlop and M. Benmalek, J. Vac. Sci. Technol., **A13**, 260 (1995).
13. F. M. Fowkes, D. W. Dwight, D. A. Cole, T. C. Huang, J. Non-Cryst. Sol., **120** , 47 (1990).
14. Y. Leterrier, J. Andersons, Y. Pitton and J.-A. E. Manson, J. Polym. Sci., part B: Polym. Phys. **35**, 1463 (1997).

CLICK TO RETURN TO LIST OF PAPERS AND PRESENTATIONS